Journal of Materials Chemistry A

ARTICLE

UV-curable fluoropolymers crosslinked with functional fluorescent dyes: the way to multifunctional thin-film luminescent solar concentrators

Received 00th January 20xx,
Accepted 00th January 20xx

DOI: 10.1039/x0xx00000x

www.rsc.org/

Diego Pintossi[a], Alessia Colombo[b], Marinella Levi[a], Claudia Dragonetti[b], Stefano Turri[a], and Gianmarco Griffini[a]*

A novel photo-curable multifunctional luminescent system with high-durability is presented in this work for application in thin-film luminescent solar concentrators (LSC), based on a fluorinated polymer matrix covalently linked to a newly synthesized functional perylene-derived luminescent organic dye. The UV-curable fluoropolymeric matrix consists in a blend of three different UV-curable fluorinated polymers. Such matrix was co-reacted upon UV-light exposure with a suitably functionalized perylene-based luminescent organic dye bearing lateral carbon double bonds, to yield the solid crosslinked LSC thin film. A thorough characterization of the new luminescent system evidenced its excellent chemical, physical and optical properties, while its functional performance was evaluated in terms of LSC device response at varying dye concentrations. To assess the long-term stability of the new UV-curable LSC system, a long term (> 800 h) light-exposure durability study was conducted on LSC devices that fully retained their initial performance. On the contrary, reference host/guest luminescent systems based on the same UV-curable fluoropolymeric matrix doped with a conventional fluorescent dye exhibited an overall ~10% efficiency loss in the same timeframe. In addition, such novel UV-curable fluoropolymeric LSC system presented highly-hydrophobic character and moderate oleophobicity, which impart easy cleanability to the LSC coating, as a result of the highly perfluorinated nature of the polymeric matrix. This study represents the first demonstration of highly-stable multifunctional UV-curable thin-film LSC systems and gives a clear demonstration of a straightforward room-temperature preparation process that may offer an easily scalable approach to highly stable and multifunctional LSC devices.

Introduction

In the field of solar energy, the use of polymer-based luminescent solar concentrators (LSCs) represents a promising strategy to improve the diffuse light response of conventional photovoltaic (PV) devices and to concentrate light without the need for expensive tracking equipment.[1] In addition, thanks to their light-weight combined with the possibility to modulate their shape and color, LSCs offer the potential to integrate PV technology in the built environment and in urban applications.[2-4] LSC systems are typically characterized by two different device architectures, namely thin-film and bulk-plate LSCs.[5-7] In both cases, a matrix material (typically polymeric) in the form of a slab (bulk configuration) or of a thin coating on a transparent substrate (thin-film configuration) embeds luminescent molecules that act as downshifting centers of the incident light. Owing to the difference in refractive indexes between LSC material and surrounding medium (*viz*., air), downshifted light can be guided by total internal reflection towards the edges of the LSC device, where it is concentrated and ultimately collected by small area solar cells.[8-11] Although the two LSC configurations are found to exhibit similar performance in terms of power conversion efficiency, thin-film devices may present some technological advantages over the bulk-plate architecture as they potentially give access to a broader range of coating techniques (e.g., spin coating, blade coating, spray coating, brush painting) and are open to a wider range of transparent substrates (both glass and plastic).[12]

In the past decade, research efforts have been largely focused on improving the solar-to-electricity conversion efficiency of LSC systems by designing new performing luminescent species and by engineering the device assembly in the attempt to bridge the gap between laboratory demonstrations and commercial exploitation.[13,14] However, to prove real commercial viability of this technology, sufficient device

[a] *Department of Chemistry, Materials and Chemical Engineering "Giulio Natta", Politecnico di Milano, Piazza Leonardo da Vinci 32, 20133 Milano, Italy. E-mail: gianmarco.griffini@polimi.it*
[b] *Department of Chemistry, Università degli Studi di Milano, Via Golgi 19, 20133 Milano, Italy.*

Electronic Supplementary Information (ESI) available: full synthetic procedure for XL-red preparation; UV-curable coating formulations; wettability behaviour of UV-curable coating; examples of luminescent systems deposited onto temperature-sensitive plastic substrates; calculation of figure of merits for dyes; optical properties of luminophores in solution and in film; thermolytic response of luminescent systems; device performance evaluation; current-voltage characteristics of solar cell and LSC; spectral response of silicon PV cell; thermogravimetric analysis and differential scanning calorimetry on aged LSCs. See DOI: 10.1039/x0xx00000x

lifetime is also required, so as to guarantee stable response during operation. In this respect, one critical aspect affecting the lifetime of LSC devices is represented by the degradation of the luminescent species.[15-17] To date, fluorescent organic dyes are the most commonly employed luminophores in the LSC field, with perylene-based systems (e.g., Lumogen F Red 305 by BASF) currently representing the materials-of-choice thanks to their high luminescence quantum yield (LQY), good compatibility with a wide range of polymeric matrices, and relatively broad absorption and emission spectra.[18] Notwithstanding these excellent characteristics, this class of materials is also characterized by relatively limited photo-stability, especially when exposed in air to the high energy portion of the solar spectrum.[19] In this respect, some possible degradation pathways have been recently proposed describing the effect of prolonged interaction of these molecules with UV light that ultimately leads to disruption of their molecular structure, reduced LQY and decreased device performance.[15] Such photo-oxidative instability is partly the result of the non-covalent interactions between polymeric carrier matrix and dye molecules, the latter being typically incorporated as guest species in the free volume of the polymeric host material, thereby allowing for relatively high molecular mobility and more expedite radical-induced molecular degradation.[20] In view of these limitations, synthetic approaches aimed at developing organic dyes suitable for covalent attachment to the polymeric matrix would be desirable, as they are expected to result in improved luminophore/matrix intrinsic stability and ultimately yield enhanced device operational lifetime.

Together with dye photodegradation, the limited stability of polymeric matrix materials under continuous illumination represents another critical factor affecting LSC lifetime. Currently, the state-of-the-art matrix material for LSC applications is poly(methyl methacrylate) (PMMA) due to its transparency in the visible range of the solar spectrum, its relatively high refractive index and the ease of processing.[19] However, PMMA exhibits relatively limited outdoor stability, especially when employed in the form of thin film, thus potentially affecting the lifetime of devices.[21,22] In particular, degradation of the polymeric matrix material may lead to the formation of photon trapping sites, which could ultimately hamper light transport towards the edges of the LSC, thereby limiting the efficiency of the system.[23,24] In addition, radical species may form as a result of the degradative processes occurring to the polymeric matrix upon light exposure that can potentially interact with the luminescent organic dye molecules, causing their degradation or negatively affecting their LQY.[25] Consequently, the quest for alternative matrices which are intrinsically stable under continuous light exposure still represents an active and ongoing research area in the field of LSC devices.

In previous works by our research group,[26,27] it was demonstrated that some specific fluorinated polymers thermally cured with different crosslinking agents may represent a viable alternative to PMMA as high durability polymeric matrices that can retain good compatibility with luminescent dyes. Indeed, LSC devices based on such fluoropolymers doped with commercial fluorescent dyes were shown to exhibit higher stability under continuous illumination compared with devices incorporating PMMA as carrier matrix, as a result of the excellent stability of the carbon-fluorine bond, which imparts remarkable durability and chemical stability to these materials.[28,29] Despite such promising results, the widespread applicability of these systems is however hindered by the high processing temperatures (≥ 150 °C) and long processing times (≥ 30 min) required for the thermal curing of the polymeric matrix, which effectively rule out the possibility to employ transparent plastic substrates. Indeed, PMMA and polycarbonate (PC, another common host matrix material for LSCs) have glass transition temperatures (*Tg*) which lie below or close to the curing temperature of these fluorinated systems, potentially giving rise to non-negligible thermally-induced distortions of the materials during the curing process.

In the present work, a detailed investigation of a novel photo-curable multifunctional luminescent system for LSC applications is presented based on a fluorinated polymer matrix covalently linked to a newly synthesized functional perylene-derived luminescent organic dye. The UV-curable fluoropolymeric matrix was obtained by formulating a modified chlorotrifluoroethylene-vinylether (CTFE-VE) copolymer with a perfluoroacrylate (PFA) monomer and a perfluoropolyether (PFPE)-urethane dimethacrylate (UDM) copolymer. Such matrix was co-reacted upon UV-light exposure with a suitably functionalized perylene-based luminescent organic dye to yield the solid crosslinked LSC thin film. A thorough chemical-physical characterization of these new LSC materials is presented and their functional device performance is evaluated at varying dye concentration. Furthermore, a long term (> 800 h) light-exposure durability study is performed on LSC devices to demonstrate the superior stability of such new co-crosslinked luminescent system compared to reference host/guest systems. In addition to the high stability and the suitable optical response, the novel system reported herein exhibits highly-hydrophobic character and moderate oleophobicity that impart easy cleanability to the LSC coating, as a result of the highly perfluorinated nature of the polymeric matrix.

To the best of our knowledge, the present work represents the first example of a highly-stable multifunctional UV-curable LSC system, and provides a clear demonstration of a straightforward and easily scalable preparation process to obtain highly hydrophobic LSC systems without the need of complex surface micro- or nanostructuring processes.

Experimental

Materials

All reagents were purchased from Sigma-Aldrich and used as received, without further purification, unless otherwise stated. A modified perylene-based organic dye was prepared (see the following section) and used for the fabrication of thin-film LSC devices. A commercial organic dye (Lumogen F Red 305 by

BASF, from here on referred to as LR305) was also used as a reference during weathering experiments. To prepare the polymeric matrix for LSC devices, Lumiflon LF-910LM (AGC Chemicals Americas), a chlorotrifluoroethylene-vinyleter (CTFE-VE) copolymer, was modified to make it photo-curable by reacting it with isocyanate ethyl methacrylate (IEM, Showa Denko) according to a previously reported procedure, yielding a UV-curable binder called UV-resin.[30-32] *1H,1H,2H,2H*-perfluorodecyl acrylate (PFA) and a perfluoropolyether-urethane dimethacrylate (PFPE-UDM) copolymer (Fluorolink MD 700, Solvay) were mixed with the modified CTFE-VE to achieve the final formulation of the polymeric matrix. Darocur 1173 (Ciba) was used as radical photoinitiator for the UV-curing process.

Synthesis of modified perylene (XL-red)

The novel *1,6,7,12-tetrakis(4-vinylphenoxy)-N,N'-(2,6-diisopropylphenyl)perylene-3,4,9,10-tetracarboxydiimide* (from here on referred to as XL-red) was achieved following the three-step procedure reported in Scheme 1.

The synthesis starts with the chlorination of 3,4:9,10-perylene tetracarboxylic dianhydride followed by reaction with 2,6-diisopropylaniline to give **2**. Subsequently, the tetrakis(vinylphenoxy)perylene-derivative (XL-red) could be prepared directly from **2** by reaction with 4-vinylphenol in presence of anhydrous K_2CO_3 in 1-methyl-2-pyrrolidone (NMP). A detailed explanation of the synthetic steps is provided in the ESI.

Coating formulation

The polymeric matrix was formulated by mixing the UV-resin with PFA monomer and PFPE-UDM with 0.73:0.18:0.09 weight ratios (several other formulations were prepared and assessed in a preliminary screening, as reported in Table S1 of the ESI). Then, the mixture was diluted in chloroform to obtain a solution with 30 wt. % dry content. The organic dye was added to the solution (0.5, 2, 3, 4, 5, 6 wt. % with respect to the dry polymer), which was left under magnetic stirring in the dark for 2 h.

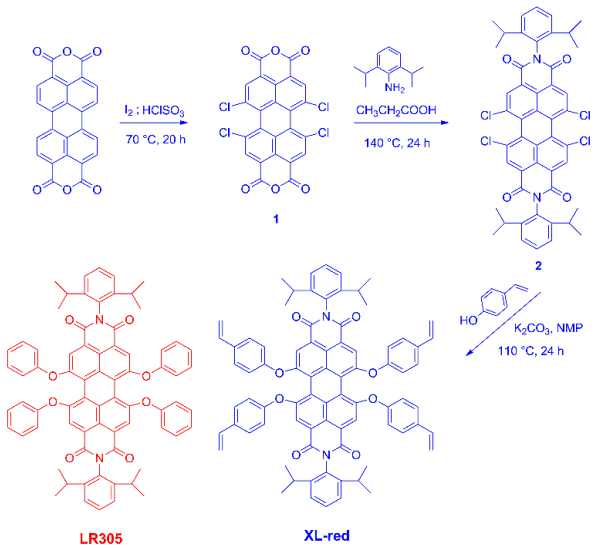

Scheme 1 Illustration of the three-step procedure leading to the synthesis of 1,6,7,12-Tetrakis(4-vinylphenoxy)-N,N'-(2,6-diisopropylphenyl)perylene-3,4,9,10-tetracarboxdiimide (XL-red). The chemical structure of Lumogen F Red 305 (LR305) is reported here for a direct comparison.

Prior to the deposition on the substrate, the photoinitiator was added to the solution with a 3 wt. % concentration with respect to the dry polymer content and allowed to undergo magnetic stirring in the dark for 10 min.

Instrumentation

Fourier-transform infrared (FTIR) spectroscopy was performed in transmission mode in air at room temperature with a FT/IR-615 spectrophotometer (Jasco Inc.) to evaluate the progress of the functionalization reaction. FTIR spectra were taken using NaCl round crystal disks. UV-visible spectroscopy analyses were performed in air at room temperature with an Evolution 600 UV-vis spectrophotometer (Thermo Scientific). Fluorescence spectra were measured in air at room temperature by using a Jasco FP-6600 Spectrofluorometer. The excitation wavelength was 445 nm. Differential scanning calorimetry (DSC) analyses were performed by means of a DSC 823e (Mettler-Toledo) instrument. The measurements consisted of three runs (heating/cooling) from 25 °C to 200 °C at 20 °C min^{-1}. To investigate the crosslinking kinetics and the reaction conversion of the photo-curable LSC coatings, photo-calorimetric analyses (photo-DSC) were performed on a DSC/823e (Mettler Toledo) coupled to a fiber-guided UV light source in the 300–450 nm wavelength range at an intensity of 15 mW cm^{-2} generated by a medium-pressure mercury lamp (Lightningcure LC8, Hamamatsu). Samples of the UV-curable matrix formulation were partially cured under UV light (Mercury vapor lamp GR.E. 500 W equipped with a Zs type light bulb, by Helios Italquartz) at increasing exposure times, then they were weighted and placed under the UV source of the photo-DSC instrument to complete the curing process while registering the residual heat flow. Thermo-gravimetric analysis (TGA) was performed both under air and nitrogen flux with a TGA Q 500 (TG Instruments). Static optical contact angle measurements on the LSC coating were performed with an OCA 20 (DataPhysics) equipped with a CCD photo-camera and with a 500-µL Hamilton syringe to dispense liquid droplets. Measurements were taken at room temperature *via* the sessile drop technique. At least 20 measurements were performed in different regions on the surface of each coating and results were averaged. Water, diiodomethane, and Nujol (mineral oil) were used as probe liquids. Coating depositions were performed with a WS-650MZ-23NPP (Laurell) spin coater on different transparent substrates (glass, PMMA, PC, poly(ethylene terephthalate) – PET). LSC devices were fabricated on glass. Testing of the LSC devices was performed under 1 sun AM1.5G illumination, provided by a Sun 2000 solar simulator (ABET Technologies) and by using a Keithley 2612B source-measuring unit to carry out the voltage scans. Data presented for each condition were averaged on at least three devices. External quantum efficiency (EQE) measurements on Si-PV devices were performed using a PVE300 Bentham (UK) station (spectral range: 300-1100 nm). LSC devices were subjected to weathering tests under continuous Xenon light illumination in a weather-o-meter chamber (Solarbox 3000e, Cofomegra S.r.l.) equipped with an

outdoor filter cutting all wavelengths below 280 nm. The total irradiance was measured by means of a power-meter with thermopile sensor (Ophir) and found to be approximately 1000 W m^{-2} (550 W m^{-2} in the 300–800 nm wavelength range) for the entire duration of the test (> 550 h). The UV-light irradiance level in the 295–400 nm range was 50 W m^{-2}, as measured by means of a UV-photodiode. The relative humidity and the working temperature inside the test chamber were maintained constant and measured to be 20% and 38 °C, respectively. The black standard temperature (BST) was 65 °C for the entire duration of the test.

Device fabrication and testing

Glass substrates (2 x 2 x 0.5 cm) were successively washed in an ultrasonic bath with water, acetone, and 2-propanol for 10 min, then they underwent an air plasma treatment for 5 min. The fluorinated matrix solution containing the organic dye was spin-cast on clean substrates in air (1200 rpm, 40 s) and cured under a UV-A lamp (Mercury vapor lamp GR.E. 500 W equipped with a Zs type light bulb, by Helios Italquartz) for a max of 5 min in a nitrogen atmosphere, thus producing a fluorescent film 1.42 ± 0.07 µm thick. The substrates coated with the luminescent system were coupled to a silicon PV cell (IXOLAR SolarBIT KXOB22 12X1 F, active area 1.2 cm^2, by IXYS - Voc = 0.64 ± 0.01 V, Isc = 42.60 ± 0.42 mA, FF = 69.4 ± 0.3 %, PCE = 15.69 ± 0.23 %) so that one edge of the concentrator was bonded to the photoactive area of the solar cell. Since the side of the glass slab was 20x5 mm^2 and the solar cell active area was 20x6 mm^2, the excess active area which was not coupled to the concentrator was covered with black tape during all characterizations. Bonding was carried out by means of a thermosetting EVA-based adhesive, which was placed on the PV cell and heated to 140 °C on a hot plate to achieve softening of the adhesive. Then, the coated glass slab was pressed onto the adhesive to grant good optical contact between the solar cell and the concentrator. Once the LSC device had cooled down to room temperature, it was ready for handling and electrical testing, which was carried out in the presence of a white back reflector. The geometric gain (G) in this configuration is 3.33. For the weathering test, LSC devices based on XL-red were prepared at a concentration of 4 wt. %. For benchmarking purposes, LSC devices based on the photocurable fluoropolymeric matrix developed here and incorporating LR305 as luminescent species were also tested. In this case, LR305 concentration (3 wt.%) was chosen so as to yield equivalent absorbance values as XL-red based systems at the maximum absorption wavelength.

Results and Discussion

The novel UV-curable luminescent system presented in this work is obtained by first formulating a methacrylate-functionalized fluoropolymeric binder (the UV-resin) with PFA and a PFPE-UDM copolymer, and it is the result of an extensive preliminary investigation on different coating formulations (see Table S1 of the ESI) aimed at the selection of the most promising coating material for LSC application. Such selection was based on four main criteria: high luminophore solubility in the matrix, prolonged outdoor durability, high hydrophobicity and high optical transmittance. Accordingly, the fluorinated UV-resin was chosen due to its excellent photo-chemical stability accompanied by its intrinsic transparency, ease of crosslinking and excellent compatibility with aromatic molecules, such as organic dyes. PFPE-UDM was added to the UV-resin to enhance the hydrophobic character and the surface activity of the resulting solid film, in the attempt to produce a coating material also embedding an easy-cleanability functionality. PFA was selected to act as compatibilizing agent between the UV-resin and the PFPE-UDM to enable elevated optical transmittance throughout the visible spectrum. To impart the optical functionality to the fluoropolymeric film, such matrix was co-reacted upon UV-light exposure with a functionalized perylene-based luminescent organic dye (XL-red, Scheme 1) previously dissolved in the matrix precursor solution, yielding the solid luminescent thin film. In the presence of a suitable photoinitiator, the C=C moieties synthetically attached to the phenoxy groups in *bay*-positions in XL-red enable UV-induced radical-mediated crosslinking reaction with the acrylate and methacrylate groups present in the matrix precursors (UV-resin, PFA, PFPE-UDM). As a result, a three-dimensional network is formed in which the luminescent dye is covalently linked to the fluoropolymeric chains, thereby reducing its molecular mobility and prospecting an improved long term photochemical stability.

To evaluate the thermal properties of the novel LSC system, DSC analysis was performed on the UV-cured luminescent coating.

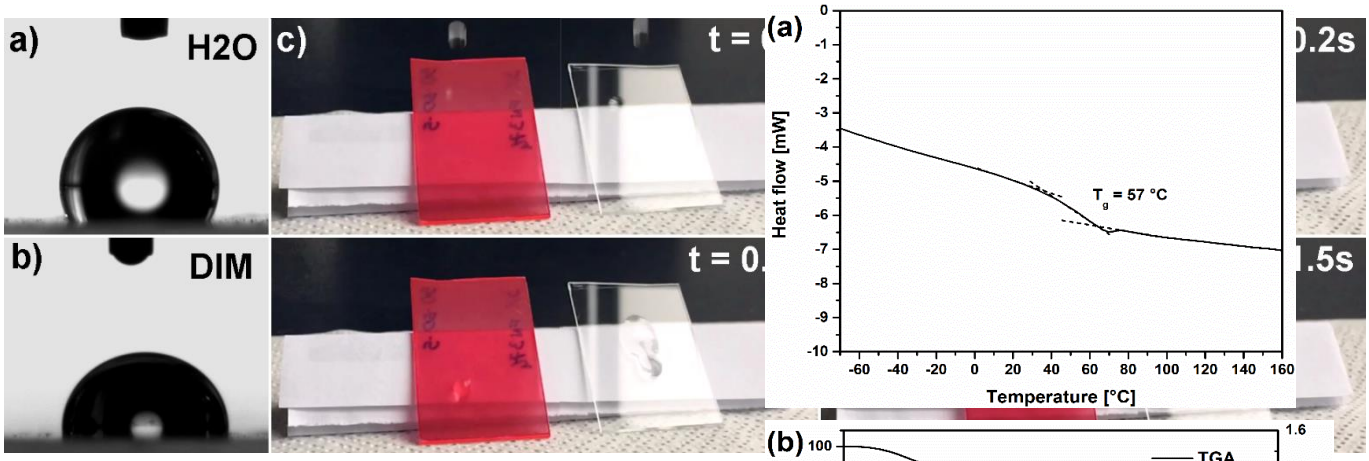

Fig. 2 a) water droplet on the fluorinated coating; b) diiodomethane (DIM) droplet on the fluorina slab coated with the luminescent fluorinated system and (right) on bare glass at increasing times.

Fig. 1 (a) differential scanning calorimetry and (b) TGA curves for the luminescent coating material in air.

As shown in Figure 1a, a single *Tg* is observed at 57 °C. For LSC applications, *Tg* should be higher than room temperature so as to prevent flow of the polymeric film due to increased macromolecular mobility, thus limiting physical degradation of the matrix during operating conditions. Accordingly, the high value of *Tg* of this LSC system suggests its suitability for outdoor use. In addition, the presence of a single *Tg* value provides a clear indication of the monophasic nature of the investigated polymeric system, thus demonstrating the excellent miscibility between the fluorinated components of the LSC matrix (UV-resin, PFA and PFPE-UDM).

The thermal stability of the crosslinked fluorinated LSC system was investigated by means of TGA in air (Figure 1b). The thermo-oxidative response of the luminescent material is characterized by the presence of three peaks in the differential weight loss curve. The first peak at 150 °C may be associated with decomposition of urethane linkages. The second peak at 385 °C may be related to the decomposition of ether and ester linkages. Finally, the third peak at 530 °C may be caused by the complete degradation and depolymerization of the material. Similar trends were observed also in thermolytic conditions (see ESI for TGA under nitrogen flux). As a result, considering the typical service temperatures of LSC systems in urban environments (well below 50 °C, depending on the geographical location),[33] the fluorinated material exhibits a satisfactory thermal stability for LSC applications.

An investigation into the wettability behavior of the LSC coating was performed by measuring the static contact angles of the luminescent thin film with different liquids, namely water, diiodomethane, and Nujol. The surface energy, with its dispersive and polar components, was calculated using the Owens, Wendt, Rabel, and Kaelble (OWRK) method (the complete results are listed in Table S2 in the ESI).[34-36]

The crosslinked luminescent coating exhibits a remarkably high value of water static contact angle (119.4° ± 0.7°). To the best of our knowledge, this represents to date the highest water contact angle value on polymeric LSCs obtained without integrating micro- or nanostructured architectures on the coating surface. Within this context, it is worth noting that such pronounced hydrophobic behavior was obtained by means of a relatively simple approach (UV-induced crosslinking) that lends itself to a straightforward scalability in view of the successful incorporation of LSC devices in building integrated PV (BIPV) applications. The poor water wettability of this novel LSC system appears even more significant if compared to the most commonly employed PMMA, which instead exhibits a clearly hydrophilic behavior with a static water contact angle of about 70°.[27,37] In addition to the remarkable hydrophobicity, the system also exhibits a relatively high static contact angle with diiodomethane (> 100°) and mineral oil (Nujol) (> 90°), thus indicating its moderate oleophobic behavior. The static contact angles and the low value of the surface energy of the coating, with a low polar component typical of fluorinated systems, provide the coating with an easy-cleaning functionality, preventing the accumulation of dirt and solid particles on the LSC surface during operation (see ESI). This highly hydrophobic behavior is evident in the sequence of pictures in Figure 2, which depicts the behavior of a water droplet falling on the luminescent fluorinated coating system as compared to an uncoated bare glass slide. This short sequence of still frames (the full original movie is available in the ESI) clearly highlights the potential easy-cleaning functionality of the new fluorinated LSC system, which enables a much faster water droplet sliding (~ 5x) compared with uncoated glass.

To evaluate the optical characteristics of the LSC coating, a photophysical characterization of the newly synthesized XL-red was performed by means of UV-vis and fluorescence spectroscopy. The resulting spectra are reported in Figure 3, where the optical response of the commercial perylene-based dye LR305 (Scheme 1) is also reported for reference. Both fluorescent systems exhibit two main absorption peaks. As demonstrated in previous works,[15] the longer wavelength peak can be attributed to the absorption of the perylene core, while the peak at shorter wavelengths can be associated with the absorption of the phenoxy groups in *bay*-positions on the dye molecule. In addition, the long wavelength peak is slightly redshifted for XL-red compared to LR305, likely due to the increased conjugation length resulting from the addition of the C=C moieties in the new system. The absorption and emission spectra of the two dyes, together with the external quantum efficiency (EQE) of the solar cells used to fabricate the LSC devices (see the following paragraphs for the description of device response and the ESI for EQE measurements), were employed for the calculation of four characteristic figures of merit (FoM) useful to assess the optical matching between luminophore, PV cell and solar emission spectrum, namely radiative overlap (RO), parasitic absorption (PA), absorption spectral matching (ASM), and emission spectral matching (ESM).[38] Such FoM are quantitative indexes that enable a direct comparison of the performance of different dyes potentially eligible for LSC applications. The two luminescent systems exhibit fairly similar values for the various FoM (see ESI for a detailed description of the FoM and the complete list of their values for the two dyes). However, ASM was found to be sensibly higher for XL-red than for LR305.

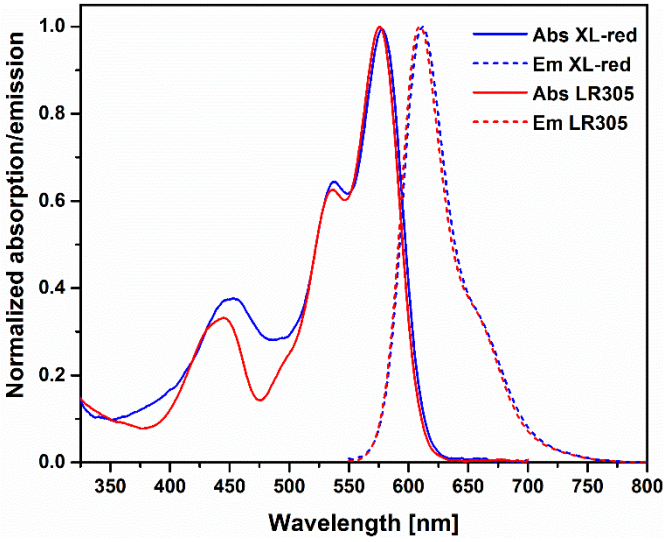

Fig. 3 Absorption and emission spectra of the dyes: (red) LR305 and (blue) modified co-crosslinkable perylene XL-red.

Such notable difference may be explained by taking into account the different relative intensities of the absorption peaks for XL-red and LR305 in the short wavelength spectral region. In the case of XL-red the slightly higher and broader response in the < 500 nm wavelength region may enable the absorption of a larger number of solar photons not optimally utilized by the PV cell, thus resulting in better exploitation of the incident solar spectrum.

An evaluation of the UV-mediated crosslinking kinetics of the luminescent fluorinated system and on the influence of the presence of XL-red on the crosslinking conversion was carried out by means of photo-DSC measurements. The conversion curve of the photo-crosslinking process for the fluorinated coating (undoped and doped with XL-red) irradiated at increasing exposure times was constructed by computing the ratio between the residual enthalpy of reaction at different UV pre-exposure times to the heat of reaction of the uncured LSC precursor mixture. The resulting curves for the undoped and doped fluorinated systems are reported in Figure 4a.

It can be noted that the presence of XL-red in the coating slows down lightly the crosslinking process, due to the competitive absorption which takes place between photoinitiator and luminophore. However, the longer curing times for the doped systems compared to the transparent matrix (140 s vs. 60 s to achieve > 99% conversion in doped and undoped systems, respectively) are still largely compatible with a potential upscale of the process. Furthermore, it is worth noting that the curing time can be easily reduced by appropriately modulating the incident power density of the UV-light source.

To further investigate the crosslinking behavior of the doped and undoped systems, FTIR spectra measurements of the coatings before and after irradiation with UV light were performed. The resulting spectra (Figure 4b) provide an additional confirmation that the conversion of the coating is not affected by the presence of the dye, as the peak associated to the carbon-carbon double bonds in the polymeric precursor formulation (acrylate and methacrylate groups in UV-resin, PFA and PFPE-UDM; pendant C=C moieties in XL-red) visible at 1640 cm^{-1} is found to completely disappear upon UV-irradiation in the case of both doped and undoped systems. In addition, this evidence further demonstrates successful covalent incorporation of XL-red into the fluoropolymeric matrix network, as no residual C=C signals are found in the FTIR spectrum of doped systems after complete crosslinking.

As additional proof of the chemical bonding occurring between XL-red and polymeric matrix, solvent extraction tests were performed on LSC coatings by means of suitable solvents capable of swelling the undoped polymeric matrix (e.g., chloroform or toluene). In this respect, successful covalent bond formation between dye and polymer network should prevent extraction of the luminophore due to impaired molecular mobility of the dye. Based on these considerations, LSC films incorporating XL-red were immersed in either chloroform or toluene and no dye leaching was observed even after prolonged immersion times (> 10 min), as expected. On the contrary, full discoloration of the luminescent coating was observed after less than 10 s of solvent immersion in the case of the novel fluorinated matrix doped with LR305, proving that complete extraction of the dye molecule occurs in host/guest systems.

To prove the wide applicability of the room-temperature process presented in this work, the new UV-curable fluoropolymeric luminescent coatings were also deposited on different plastic substrates, namely PET, PMMA and PC. As expected, the photo-crosslinked luminescent coatings proved to fully retain their optical response with no visible distortions of the substrates after UV-treatment, thus further confirming the versatility of the approach proposed here (see ESI).

Following the characterization of the fluorinated matrix and the investigation of the photophysical properties of the reactive organic dye, LSC devices were fabricated and their PV performance was tested as a function of XL-red concentration.

Figure 5a illustrates the PV response of LSC devices fabricated

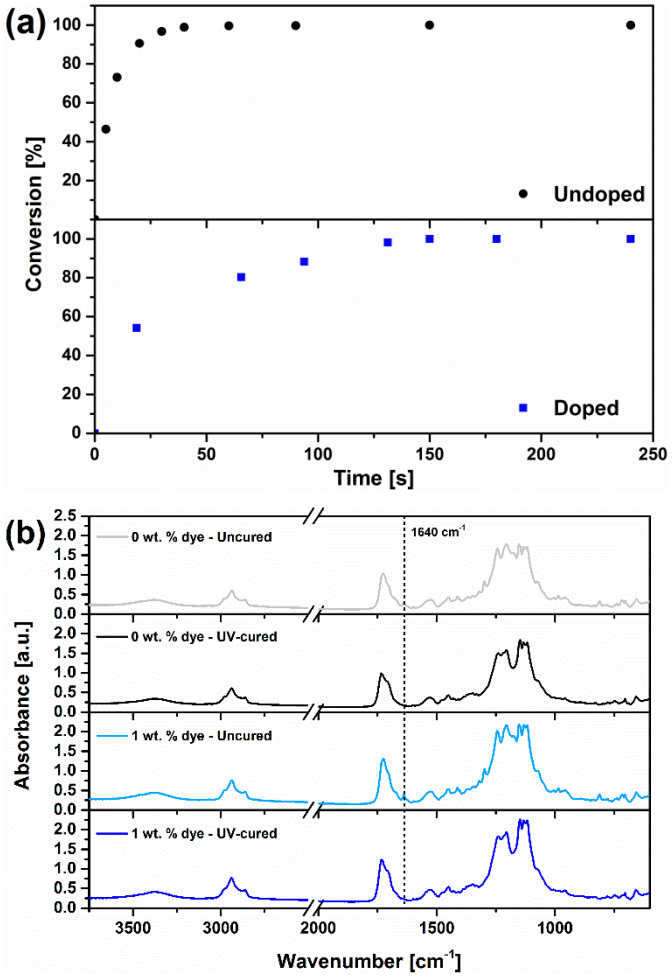

Fig. 4 (a, top) conversion over curing time curve for undoped fluorinated system and (a, bottom) conversion over curing time curve for fluorinated matrix embedding XL-red; (b) FTIR spectra before and after UV curing for both the doped and undoped fluorinated matrices.

with increasing concentrations of XL-red covalently crosslinked within the multifunctional fluoropolymeric matrix. The LSC device performance is found to progressively increase by increasing fluorophore concentration up to a maximum observed at an intermediate XL-red concentration of 4 wt. %, leading to mean values of absolute device efficiency η_{LSC}, optical efficiency η_{opt} and concentration factor C of 1.98%, 13.9% and 0.46, respectively (see ESI for details and definitions of η_{LSC}, η_{opt} and C). This trend may be correlated with the progressively higher optical density of the film (i.e., larger number of dye molecules) with increasing fluorophore concentration that results in a higher fraction of incident photons to be absorbed, reemitted and made available to the PV cell for photon-to-current conversion. By increasing further dye concentration (> 4 wt. %), a sharp performance decrease is observed. This behavior can be related to the progressively higher probability for reabsorption phenomena to occur in the LSC thin film before emitted photons can reach the edge-mounted PV cells, as a result of the decreasing dye-to-dye

intermolecular distance and the partial overlap between absorption and emission spectra of the dye.[39]

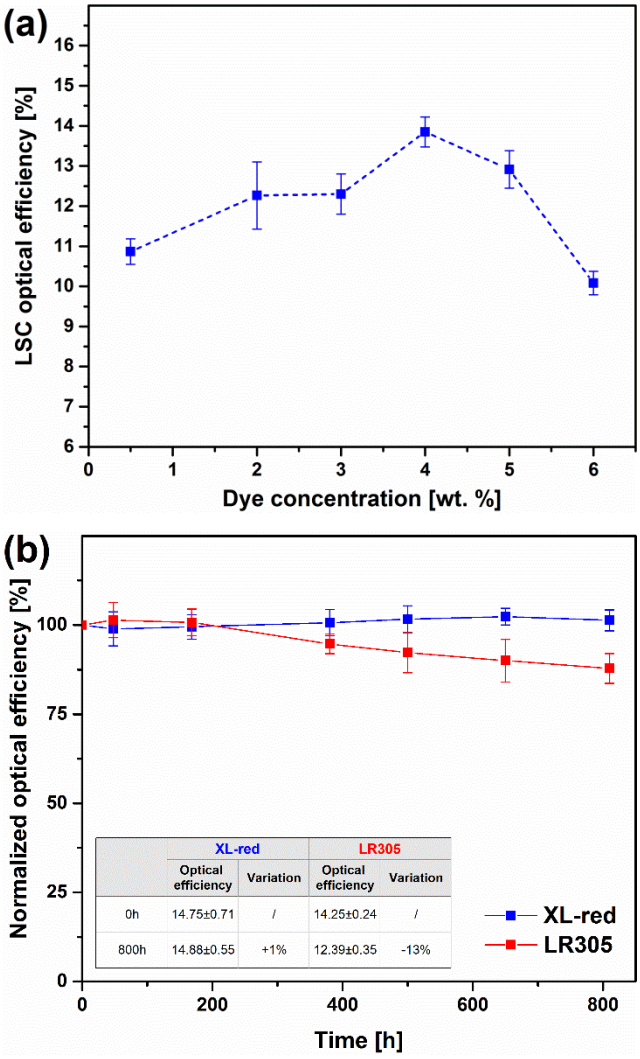

Fig. 5 (a) optical efficiency of the LSC devices with increasing concentration of XL-red embedded in the fluorinated matrix; (b) normalized optical efficiency over time during the weathering test for LSC systems based on XL-red and on LR305.

It is worth noting that the values of η_{LSC}, η_{opt} and C obtained in this work are consistent with those available in recent LSC literature,[40-42] despite the main focus of the present work was on improving the stability and increasing the functionality of LSC devices. Further improvements of the photon-to-current performance may be attained by additional device optimization (e.g., use of mirrors on the free edges of the LSC device), which is however beyond the scope of this work. Based on these considerations, these results confirm the suitability of XL-red as a valid alternative to LR305 in the fabrication of high performance LSCs.

To assess the long-term stability of the new UV-curable LSC system, devices covalently incorporating XL-red as luminescent species were subjected to a prolonged (> 800 h) accelerated weathering test in the presence of continuous illumination and device performance was periodically evaluated. For comparison, LSC devices based on LR305 dissolved in the UV-curable matrix (host/guest systems) were also tested. As shown in Figure 5b, the co-crosslinked LSC system based on XL-red exhibits a stable PV behavior throughout the test with no detectable losses in optical efficiency even after more than 800 h of continuous illumination. On the other hand, the host/guest system reveals an overall ~10% efficiency loss in the same timeframe.

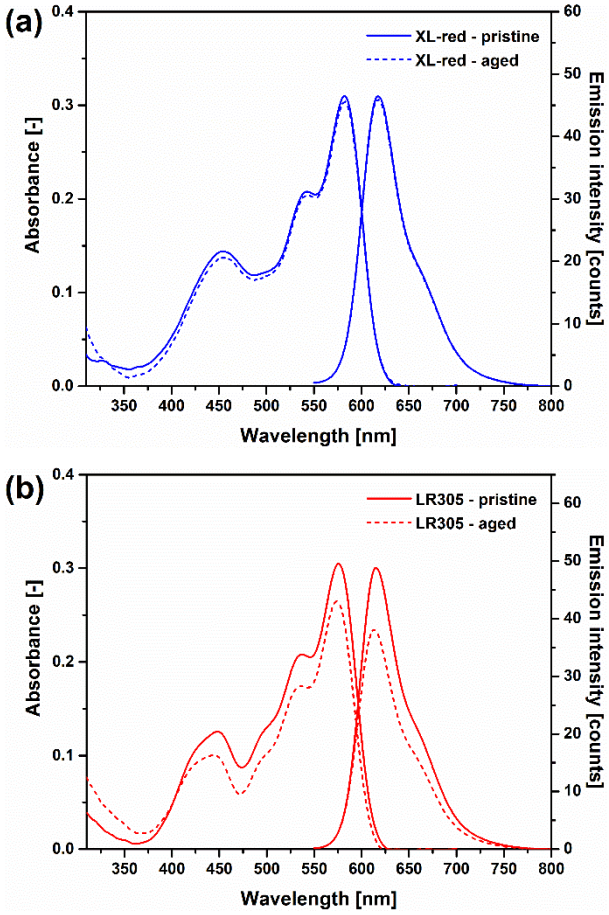

Fig. 6 Absorption and emission spectra of (a) XL-red and (b) LR305 LSC systems prior to and after weathering.

In the attempt to correlate the trends observed on device efficiency with the optical properties of the luminescent coatings, the absorption and emission response of the LSCs was evaluated prior to and after the weathering test. As shown in Figure 6, where the UV-vis and fluorescence spectra of pristine and aged luminescent coating systems are reported, different trends can be observed for LR305 and XL-red systems. In particular, the new co-crosslinked fluorophore appears to fully retain its optical properties during continuous light exposure, as no detectable modifications to the absorption and emission spectra of XL-red coatings are detected after the long-term weathering test. This behavior is

in agreement with the excellent long-term performance exhibited by the corresponding LSC devices (Figure 5). On the contrary, the system based on LR305 exhibits a decrease of absorption and emission intensity after weathering, accompanied by a 2 nm blue-shift of the maximum absorption and emission peaks (Figure 6b). This change in the optical response of LR305-based coatings may be correlated with the performance decrease experienced by LR305-based LSC devices after prolonged light exposure (Figure 5). As recently reported on the same fluorescent dye,[15] such worsening in the optical response may be ascribed to the chemical modifications occurring to the dye molecule when subjected to prolonged light exposure, thus ultimately resulting in a device response decay over time. It is also worth highlighting that no significant modifications were observed on the UV-curable polymeric matrix material upon weathering in terms of its thermal and surface wettability properties, as evident from the TGA, DSC and optical contact angle measurements carried out on this coating system after prolonged light exposure (see ESI). These trends highlight the excellent stability of the new UV-curable LSC system, in which the covalent incorporation of XL-red within the fluoropolymeric three-dimensional network results in decreased molecular mobility, thus significantly limiting radical-induced photo-degradation phenomena that may occur to the dye molecule during prolonged light exposure. As opposed to this, the non-covalent interactions between polymeric carrier matrix and dye molecules in the host/guest system allow relatively higher molecular mobility and more expedite radical-induced molecular degradation processes, ultimately leading to poorer photo-oxidative stability and decreased device performance over time. This behavior is in line with previously reported data on similar host/guest fluorinated LSC systems containing LR305 obtained by thermal curing,[27] thus confirming the key role played by the presence of a three-dimensional crosslinking network between luminescent material and polymeric matrix to hinder fluorophore degradation and fully retain LSC device response upon prolonged light exposure.

Conclusions

A novel photo-curable high-durability multifunctional luminescent system was presented in this work for applications in thin-film LSC devices. The solid luminescent coating was obtained by covalently incorporating a new functionalized perylene-based luminophore (XL-red) in a newly designed fluoropolymeric matrix upon exposure to UV-light in the presence of a suitable radical photoinitiator. A thorough characterization of the new luminescent system evidenced its excellent chemical, physical and optical properties, while its functional performance was evaluated in terms of LSC device response at varying dye concentrations. To assess the long-term stability of the new UV-curable LSC system, a prolonged (> 800 h) accelerated weathering test was conducted on devices covalently incorporating XL-red as luminescent species as well as on reference LSC devices based on a reference host/guest system. The co-crosslinked LSCs based on XL-red exhibited exceptionally stable PV response throughout the test with no detectable performance losses even after more than 800 h of continuous illumination. On the other hand, the host/guest system reveals an overall ~10% efficiency loss in the same timeframe. The excellent stability of the new UV-curable LSC system was attributed to the covalent incorporation of XL-red within the fluoropolymeric three-dimensional network that limits radical-induced photo-degradation phenomena that may occur to the dye molecule during prolonged light exposure.

In addition to the high stability and the suitable optical response, such novel UV-curable fluoropolymeric luminescent system presented highly-hydrophobic character and moderate oleophobicity, which impart easy cleanability to the LSC coating, as a result of the highly perfluorinated nature of the polymeric matrix.

In conclusion, the results of this study give a clear demonstration of a room-temperature versatile approach to readily obtain efficient, highly stable and easy-cleanable thin-film LSC devices that may find prospective use as reliable multifunctional light-harvesting systems in the urban environment.

References

1 M. G. Debije and P. P. C. Verbunt, *Adv. Energy Mater.*, 2012, **2**, 12.
2 C. Corrado, S. W. Leow, M. Osborn, E. Chan, B. Balaban and S. A. Carter, *Sol. Energy Mater. Sol. Cells*, 2013, **111**, 74.
3 G. Kocher-Oberlehner, M. Bardosova, M. Pemble and B. S. Richards, *Sol. Energy Mater. Sol. Cells*, 2012, **104**, 53.
4 J. W. E. Wiegman and E. Van Der Kolk, *Sol. Energy Mater. Sol. Cells*, 2012, **103**, 41.
5 A. Goetzberger, *Appl. Phys.*, 1978, **16**, 399.
6 A. Goetzberger and W. Greube, *Appl. Phys.*, 1977, **14**, 123.
7 W. H. Weber and J. Lambe, *Appl. Opt.*, 1976, **15**, 2299.
8 M. J. Currie, J. K. Mapel, T. D. Heidel, S. Goffri and M. A. Baldo, *Science*, 2008, **321**, 226.
9 D. J. Farrell and M. Yoshida, *Prog. Photovolt: Res. Appl.*, 2012, **20**, 93.
10 B. S. Richard and A. Shalav, *Synth. Met.*, 2005, **154**, 61.
11 G. Smestad, H. Ries, R. Winston and E. Yablonovitch, *Sol. Energy Mater.*, 1990, **21**, 99.
12 R. Bose, D. J. Farrell, A. J. Chatten, M. Pravettoni, A. Buchtemann and K. W. J. Barnham, in Proceedings of the 22nd European Photovoltaic Solar Energy Conference, Milan, 2007, 210.
13 J. Lucarelli, M. Lessi, C. Manzini, P. Minei, F. Bellina and A. Pucci, *Dyes Pigm.*, 2016, **135**, 154.
14 F. Bellina, C. Manzini, G. Marianetti, C. Pezzetta, E. Fanizza, M. Lessi, P. Minei, V. Barone and A. Pucci, *Dyes Pigm.*, 2016, **134**, 118.
15 G. Griffini, L. Brambilla, M. Levi, M. Del Zoppo, S. Turri, *Sol. Energy Mater. Sol. Cells*, 2013, **111**, 41.
16 N. Tanaka, N. Barashkov, J. Heath and W. N. Sisk, *Appl. Opt.*, 2006, **45**, 3846.
17 A. A. Earp, T. Rawling, J.B. Franklin and G. B. Smith, *Dyes Pigm.*, 2010, **84**, 59.
18 L. R. Wilson and B. S. Richards, *Appl. Opt.*, 2009, **48**, 212.
19 W. G. J. H. M. Van Sark, K. W. J. Barnham, L. H. Slooff, A. J. Chatten, A. Büchtemann, A. Meyer, S. J. McCormack, R. Koole, D. J. Farrell, R. Bose, E. E. Bende, A. R. Burgers, T. Budel, J. Quilitz, M. Kennedy, T. Meyer, C. De Mello Donegá,

A. Meijerink and D. Vanmaekelbergh, *Opt. Express*, 2008, **16**, 21773.
20 A. Dubois, M. Canva, A. Brun, F. Chaput and J.-P. Boilot, *Appl. Opt.*, 1996, **35**, 3193.
21 H. Kaczmarek, A. Kamińska and A. Van Herk, *Eur. Polym. J.*, 2000, **36**, 767.
22 B. Ranby and J. F. Rabek, *Photodegradation, Photo-oxidation and Photostabilization of Polymers: Principles and Applications*, John Wiley & Sons Ltd., London, 1975.
23 J. C. Goldschmidt, M. Peters, M. Hermle and S. W. Glunz, *J. Appl. Phys.*, 2009, **105**, 114911.
24 R. Sóti, E. Farkas, M. Hilbert, Z. Farkas and I. Ketskeméty, *J. Lumin.*, 1996, **68**, 105.
25 I. Baumberg, O. Berezin, A. Drabkin, B. Gorelik, L. Kogan, M. Voskobojnik and M. Zaidman, *Polym. Degrad. Stab.*, 2001, **73**, 403.
26 G. Griffini, M. Levi and S. Turri, *Sol. Energy Mater. Sol. Cells*, 2013, **118**, 36.
27 G. Griffini, M. Levi and S. Turri, *Prog. Org. Coat.*, 2014, **77**, 528.
28 D. M. Lemal, *J. Org. Chem.*, 2004, **69**, 1.
29 G. Griffini and S. Turri, *J. Appl. Polym. Sci.*, 2016, **133**, 43080.
30 G. Griffini, F. Bella, F. Nisic, C. Dragonetti, D. Roberto, M. Levi, R. Bongiovanni and S. Turri, *Adv. Energy Mater.*, 2015, **5**, 1401312.
31 F. Bella, G. Griffini, M. Gerosa, S. Turri and R. Bongiovanni, *J. Power Sources*, 2015, **283**, 195.
32 F. Bella, G. Griffini, J.-P. Correa-Baena, G. Saracco, M. Grätzel, A. Hagfeldt, S. Turri and C. Gerbaldi, *Science*, 2016, **354**, 203.
33 M. C. Alonso García, J. L. Balenzategui, *Renewable Energy*, 2004, **29**, 1997.
34 D. Kaelble, *J. Adhesion*, 1970, **2**, 66.
35 D. K. Owens and R. Wendt, *J. Appl. Polym. Sci.*, 1969, **13**, 1741.
36 W. Rabel, *Farbe und Lack*, 1971, **77**, 997.
37 Y. Ma, X. Cao, X. Feng, Y. Ma and H. Zou, *Polymer*, 2007, **48**, 7455.
38 D. Alonso-Álvarez, D. Ross, E. Klampaftis, K. R. McIntosh, S. Jia, P. Storiz, T. Stolz and B. S. Richards, *Prog. Photovolt: Res. Appl.*, 2015, **23**, 479.
39 G. Griffini, M. Levi and S. Turri, *Renewable Energy*, 2015, **78**, 288.
40 Y. Li, J. Olsen, K. Nunez-Ortega, W. J. Dong, *Sol. Energy*, 2016, **136**, 668.
41 S. F. Correia, P. P. Lima, P. S. André, M. R. S. Ferreira and L. A. D. Carlos, *Sol. Energy Mater. Sol. Cells*, 2015, **138**, 51.
42 L. Desmet, A. Ras, D. De Boer and M. Debije, *Opt. Lett.*, 2012, **37**, 3087.